



2nd Advanced Optical Metrology Compendium

Advanced Optical Metrology

Geoscience | Corrosion | Particles | Additive Manufacturing: Metallurgy, Cut Analysis & Porosity



EVIDENT
OLYMPUS

WILEY

The latest eBook from **Advanced Optical Metrology**.
Download for free.

This compendium includes a collection of optical metrology papers, a repository of teaching materials, and instructions on how to publish scientific achievements.

With the aim of improving communication between fundamental research and industrial applications in the field of optical metrology we have collected and organized existing information and made it more accessible and useful for researchers and practitioners.

EVIDENT
OLYMPUS

WILEY

Light-Driven Proton Transfer for Cyclic and Temporal Switching of Enzymatic Nanoreactors

Silvia Moreno, Priyanka Sharan, Johanna Engelke, Hannes Gumz, Susanne Boye, Ulrich Oertel, Peng Wang, Susanta Banerjee, Rafal Klajn, Brigitte Voit, Albena Lederer,* and Dietmar Appelhans*

Temporal activation of biological processes by visible light and subsequent return to an inactive state in the absence of light is an essential characteristic of photoreceptor cells. Inspired by these phenomena, light-responsive materials are very attractive due to the high spatiotemporal control of light irradiation, with light being able to precisely orchestrate processes repeatedly over many cycles. Herein, it is reported that light-driven proton transfer triggered by a merocyanine-based photoacid can be used to modulate the permeability of pH-responsive polymersomes through cyclic, temporally controlled protonation and deprotonation of the polymersome membrane. The membranes can undergo repeated light-driven swelling–contraction cycles without losing functional effectiveness. When applied to enzyme loaded-nanoreactors, this membrane responsiveness is used for the reversible control of enzymatic reactions. This combination of the merocyanine-based photoacid and pH-switchable nanoreactors results in rapidly responding and versatile supramolecular systems successfully used to switch enzymatic reactions ON and OFF on demand.


such as reversible operation of molecular machines,^[25–28] switching of vesicles and nanocapsules,^[14,29–33] bioimaging of molecules and compartments,^[16,18,21,23,24,34] and dynamic self-assembly of nanoparticles and vesicles.^[5,35] In the development of “complex adaptive systems,”^[36] that is, life-like, bioinspired, intelligent, adaptive, and interactive materials, the isomerization of photochromic systems such as azobenzenes and spiropyrans is actively used for the establishment of cell mimics (e.g., liposomes with artificial or semi-synthetic channel/pore proteins) with spatiotemporal and reversible control over membrane permeability.^[1,3,4,7,10,22,29,37–40] These studies are inspired by cells as out-of-equilibrium systems that use temporal, parallel, and synchronized biological actions to move, communicate, and replicate. Moreover, previous efforts have paved the way to create self-adaptive^[41] and light-responsive, wave-length-selective^[31,32] polymersomes with switchable membrane permeability for the release of cargo and control of enzymatic reactions “on demand”. This stimulated us to search for a further simplification of self-adaptive, pH-responsive polymersomes^[41] as organelle mimics with desired out-of-equilibrium properties, leading to the concept of light-driven proton-transfer^[11,12,20,22,27] through the reversible transformation of protonated-merocyanine/spiropyran (MEH/SP) pair (Scheme 1).

1. Introduction

Over the last two decades, a plethora of light-responsive materials for different applications have been developed.^[1–24] Light is a highly attractive stimulus due to its high spatial and temporal resolution, controllability, and non-invasiveness. Owing to these characteristics, light can precisely orchestrate the isomerization, mobility, and degradation of chromophores for various processes,

Dr. S. Moreno, P. Sharan, J. Engelke, Dr. H. Gumz, Dr. S. Boye, Dr. U. Oertel, P. Wang, Prof. B. Voit, Dr. A. Lederer, Dr. D. Appelhans
Leibniz-Institut für Polymerforschung Dresden e.V.
Hohe Straße 6, Dresden 01069, Germany
E-mail: lederer@ipfdd.de; applhans@ipfdd.de

P. Sharan, J. Engelke, P. Wang, Prof. B. Voit, Dr. A. Lederer
Faculty of Chemistry and Food Chemistry
Technische Universität Dresden
Dresden 01062, Germany

 The ORCID identification number(s) for the author(s) of this article can be found under <https://doi.org/10.1002/smll.202002135>.

© 2020 The Authors. Published by Wiley-VCH GmbH. This is an open access article under the terms of the Creative Commons Attribution License, which permits use, distribution and reproduction in any medium, provided the original work is properly cited.

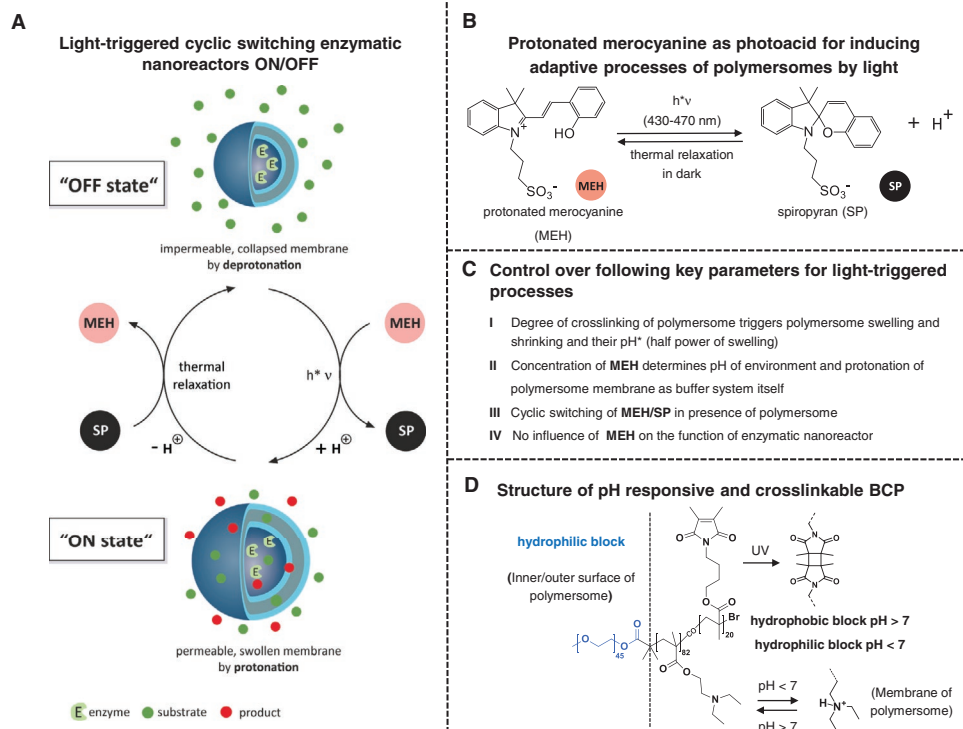
P. Sharan, Prof. S. Banerjee
Materials Science Centre
Indian Institute of Technology Kharagpur
Kharagpur 721302, India

Dr. H. Gumz, Prof. B. Voit
Center for Advancing Electronics Dresden
Technische Universität Dresden
Dresden 01062, Germany

Prof. R. Klajn
Department of Organic Chemistry
Weizmann Institute of Science
Rehovot 76100, Israel

Dr. A. Lederer
Department of Chemistry and Polymer Science
Stellenbosch University
Private Bag X1, Matieland 7602, South Africa

DOI: 10.1002/smll.202002135



Scheme 1. A) Functional principle of adaptive and cyclic opening and closing of polymersome membrane with control of the enzymatic reaction in the nanoreactor. B) Light-induced switching between protonated merocyanine (MEH) and spiropyran (SP). C) Key parameters I–IV for light-triggered processes of enzymatic nanoreactors. D) Chemical structure and composition of block copolymer (BCP) used in our experiments.^[61]

Light-driven proton transfer is widely employed by living cells and bacteria to initiate signal transduction of biological pathways.^[11,42–45] Recently, light-induced proton-pumps (LIPPs) have been unidirectionally incorporated within polymeric and liposomal vesicles to pump protons into the lumen^[46,47] or outside of the vesicles^[48] and to fabricate larger complex cellular compartments with LIPPs inducing artificial photosynthetic processes.^[49,50] Inspired by these results, light-driven proton transfer triggered by the switching of MEH/SP^[51,52] (Scheme 1) and its derivatives^[51,53,54] has been successfully applied for the temporal control of pH switches,^[51,52] proton-catalyzed reactions,^[51] proton/ion transfer through bilipid vesicles,^[38] self-assembly of nanoparticles,^[55] and proton-driven molecular machines.^[27,28,56] Moreover, this process is also involved in the cyclic spatiotemporal control over the dynamic assembly of SiO₂–Pt Janus particles^[57] and the disappearing of images with time.^[55] Visible-light irradiation of MEH induces its transformation into a stronger acid (SPH), which readily dissociates into SP and H⁺; Scheme 1B).^[51] This process typically entails a pH drop by ≈2 when starting from pH = 7, although the pH decrease is concentration-dependent and the starting pH value also plays an important role. The pH decrease is reversible and the pH goes back up due to the thermal relaxation of SP to MEH (Scheme 1B) and can be repeated for many cycles; the half-time of the proton-dissociated state is about 70 s.^[51] The use of photoacid MEH can significantly improve the function of pH-switchable nanoreactors, traditionally triggered by manual or enzymatic change of pH, as in case of enzyme-loaded polymersomes.^[41] The reversible, light-controlled proton release from MEH replaces the need for alternating addition of i) an acid

for swelling nanoreactor's membrane and ii) urea for closing nanoreactor's membrane (through urease-catalyzed hydrolysis of urea to basic ammonia).^[41] This reduced waste generation can greatly improve the stability of enzymatic nanoreactors.^[41]

It was previously reported that vesicles based on MEH-incorporating amphiphilic block copolymers (BCP) can swell upon visible light irradiation (ON state) and return back to their original vesicular size in the dark or under UV light (OFF state).^[32] This “breathable” nature of MEH-based polymeric vesicles was used for the controlled release of low-molecular weight cargo molecules.^[32] In other studies, molecular cargo release was also achieved via light-induced disassembly of polymersomes^[58] or light-induced change in membrane permeability through crosslinking.^[59,60]

Here, we demonstrate the concept of light-controlled switching of pH-sensitive polymersomes using free MEH as a proton donor (Scheme 1). For reversible switching of enzyme-loaded nanoreactors triggered by light-driven proton transfer to be possible, structural integrity and functionality of the vesicles needs to be preserved during the cyclic switching between MEH and SP. Our previous studies on cyclic switching of (multi) enzymatic reactions focused on pH- and/or temperature-responsive enzyme-loaded nanoreactors based on photo-crosslinked polymersomes (Psomes), hollow capsules, and their multicompartments.^[61–63] The main goal of this study was to develop adaptive enzymatic nanoreactors that carry out a catalytic reaction through the cyclic temporal control over the permeability of the polymersome membrane. This strategy is based on the initial addition of MEH photoacid and the reversible, “on-demand” proton release from MEH triggered by visible light (Scheme 1). The released protons protonate the tertiary amine groups within

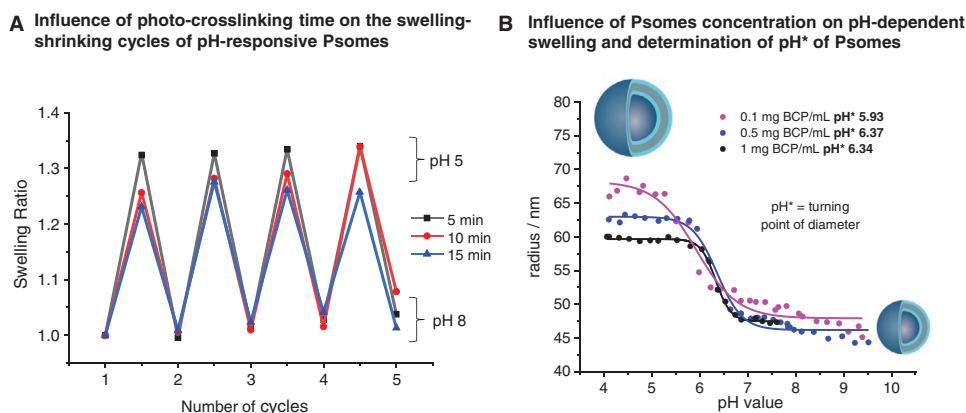


Figure 1. A) Swelling ratio of Psomes (1 mg BCP per mL)^[68] as a function of crosslinking time (key parameter I) studied by DLS. B) Influence of the Psomes concentration on the pH* value.

the polymersome membrane, rendering the membrane permeable (ON state = swollen enzymatic nanoreactor is catalytically active). When the irradiation is ceased, SP acts as a base and deprotonates the tertiary ammonium groups (Scheme 1). Consequently, the membrane returns to its impermeable state almost instantaneously (OFF state = collapsed and impermeable polymersome membrane suppresses the enzymatic nanoreactor's activity). The adaptive nature and temporally controlled function of these enzyme-loaded nanoreactors is highlighted by the fact that the back-switching occurs in the dark (thermal relaxation) and is not triggered by an additional stimulus, which constitutes a major advance compared to other pH-switchable nanoreactors reported to date. In this context, the function of the nanoreactors is validated based on two different enzymatic reactions.

2. Results and Discussion

To enable adaptive, temporal, and cyclic opening and closing of pH-switchable polymersomes' membrane on demand, several parameters of Psomes and MEH have to be studied and optimized. These parameters include concentrations of Psomes and MEH and irradiation-relaxation times of MEH/SP. In addition, it is necessary to evaluate possible interactions between vesicles' membrane and MEH (MEH itself should not affect the original properties of enzyme-loaded nanoreactors during the cyclic light-driven proton transfer). The key parameters of this study are summarized in Scheme 1.

To address the above-mentioned aims, pH-responsive BCP and the respective photo-crosslinked Psomes with pH-responsive membrane permeability for switching enzymatic reactions "ON" and "OFF" have been prepared using previously published approaches (for synthetic details and characterization of BCP, see Supporting Information).^[61,62,64,65] Molecular composition of the pH-responsive BCP is shown in Scheme 1D.

2.1. Key Parameter I: Crosslinking Time

In our previous nanoreactor studies, a crosslinking time of ≤ 180 s was used to ensure the desired swelling-shrinking behavior of the polymersome membrane, which allowed for

a reproducible control of the enzymatic reactions over many cycles.^[61,66,67] Due to the cyclic photoexcitation of MEH to SP (Scheme 1B), an increase of the crosslinking density of the membrane may happen leading to a reduction in the adaptive properties of Psomes.^[61,66,67] Therefore, the swelling-shrinking properties of Psomes after different crosslinking times (5, 10, and 15 min) were characterized by dynamic light scattering at pH 5.0 (swollen state) and pH 8.0 (shrunken state) (Figure 1, Figure S2, and Table S2, Supporting Information). Figure 1A clearly indicates that the swelling ratio is only slightly changed when the crosslinking time is increased from 5 to 15 min. Thus, 5 min of UV-crosslinking time was selected for all subsequent experiments.

2.2. Key Parameter II: Concentration of MEH and Polymersomes

The next experiments were aimed at providing the optimal concentration of MEH (Figures S4, S5, and S8, Supporting Information) and Psomes for balancing the desired effects (Figure 2), namely, efficient and reproducible pH-switchability of Psomes, optimal pH*, and reversible light-driven pH drop induced by MEH. We define pH* as the pH value, at which the Psome size changes most rapidly due to transition between the swollen and shrunken state (Figure 1B).^[67] After the validation step, the lowest BCP (0.1 mg mL^{-1}) was used to fabricate pH-responsive Psomes with a defined pH* value of 5.93 (Figure 1B), which is slightly lower than the pH* of the standardized BCP concentration (1 mg mL^{-1}) for Psomes fabrication (6.35).^[66,67] This lower Psomes concentration reduces the amount of protons that need to be liberated by MEH in order to swell the enzymatic nanoreactor under light irradiation.

In the next step, we investigated the cyclic opening (ON state) and closing (OFF state) of the polymersome membrane in the presence of MEH using visible light irradiation (Figure 2A). To this end, we first validated the applicability of light-driven proton transfer (Scheme 1) triggered by a time-dependent irradiation of MEH solution in the absence and presence of Psomes (Figures 2B,C; Figures S5 and S8, Supporting Information).^[28] This also means that the release and capture of protons by the isomerization of protonated-MEH/SP should be compatible with the protonation and deprotonation process of pH-responsive

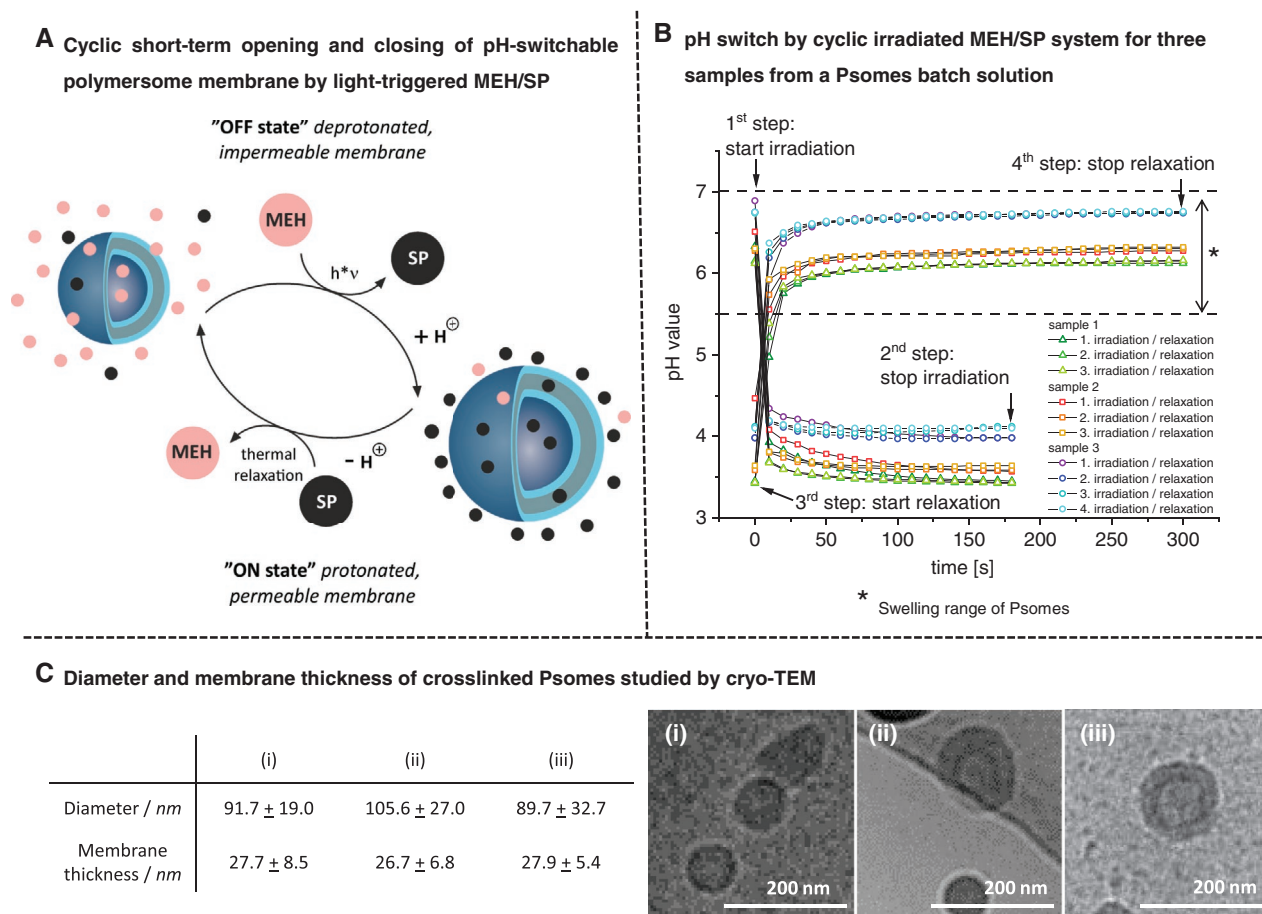


Figure 2. A) Schematic illustration of the interplay between cyclic light-triggered proton release from MEH and opening/closing of the pH-switchable polymersome membrane. B) Reversible pH changes induced by light-triggered transformation between MEH and SP after several initial irradiation–relaxation cycles in the presence of Psomes ($C_{\text{Psores}} = 0.1$ mg BCP per mL, $C_{\text{MEH}} = 1.66$ mM in MilliQ water with 5% DMSO). Three independent experiments were performed. C) Diameter and membrane thickness of Psomes in the presence of MEH i) before irradiation, ii) immediate after visible light irradiation for 3 min, and iii) after 3 min of irradiation followed by thermal relaxation for 5 min ($C_{\text{Psores}} = 0.1$ mg BCP per mL, crosslinking time = 5 min, 1.66 mM MEH). Right: the corresponding cryo-TEM images of Psomes.

Psomes (Figure 2A). We found that the reversible switching between MEH and SP was not affected by the presence of Psomes (Figure S8, Supporting Information). Furthermore, cryo-TEM imaging of Psomes ($C_{\text{Psome}} = 0.5$ mg BCP per mL, crosslinking time = 5 min) in the presence of 1 mM MEH (see, e.g., Figure S2, Supporting Information) showed that the overall size and morphology of Psomes were comparable to those reported previously.^[59–61]

To deepen our understanding of the interactions between Psomes and both states of the MEH/SP pair, Psomes were imaged by cryo-TEM in the presence and absence of MEH/SP i) before irradiation, ii) after 3 min of visible light irradiation, and iii) after 3 min of visible light irradiation followed by 5 min relaxation. Larger Psomes diameters can be expected (Figure 2A) and are detected (Figure 2C) immediately following irradiation ($\varnothing \approx 92$ nm \rightarrow $\varnothing \approx 106$ nm), with a rapid reversion to the OFF-state size ($\varnothing \approx 90$ nm) in the dark. At the same time, we found that the membrane thickness increased from 16 nm (empty polymersome in NaCl solution at pH 8) to 26–28 nm in the presence of MEH/SP for both the shrunken (MEH) and

swollen (SP) Psomes state. This finding suggests that MEH/SP is incorporated within the membrane of Psomes and/or is attached to the outer membrane of Psomes, which is confirmed by additional experiments (see Section S6, Supporting Information). Concluding this, the results also imply that the Psomes are fully stable in the presence of the MEH/SP system, and that the close association of MEH/SP with the Psomes membrane is preferentially beneficial for a substantial increase in the rate of the reversible proton transfer.

2.3. Key Parameter III: Switching of MEH/SP for Inducing Cyclic pH Changes to Control Environmental pH for the Action of Enzymatic Nanoreactors

Upon visible light irradiation of free MEH (1 mM) in the absence of Psomes, a fast pH decrease from neutral to acidic pH within 30 s takes place (Figure S8A, Supporting Information, first cycle, orange triangles). This guarantees a prompt swelling of Psomes as a result of protonation of the polymersome

membrane. Upon thermal relaxation of the system in the dark (Scheme 1), a fast (≤ 1 min) pH increase occurs, reaching stable pH values (pH > 6) within a few minutes in the dark (Figure S8A, Supporting Information, black circles). These results are in agreement with UV-vis absorption spectroscopy studies (Figure S5, Supporting Information), which show a fast response of the system and a high degree of switching reversibility (>90% over ten switching cycles) between MEH and SP both in the absence and presence (Figure S5B, Supporting Information) of Psomes.

Figure 2B shows the effect of visible light irradiation/thermal relaxation on solution pH under optimized conditions in the presence of Psomes after several initial light/dark cycles. The pH changes (neutral to acidic and back) are reversible and highly reproducible, but also in agreement with the literature results.^[17] Importantly, these results show that i) the presence of Psomes does not affect the cyclic reversible switching of the MEH/SP pair and ii) the pH change accompanying the switching process is well-suited for protonation and deprotonation of the polymersome membrane (Figure 2B).

2.4. Key Parameter IV: Influence of MEH on pH-Dependent Properties of Enzymatic Nanoreactors

As the next step toward the establishment of adaptive enzymatic nanoreactors, we studied the stability and enzymatic activity of enzyme-containing Psomes in the presence of MEH (Scheme 1, key parameter IV) under repeated irradiation-relaxation cycles. We hypothesized that exposing the nanoreactors to visible light in the presence of MEH would trigger a fast opening of the polymersome membrane and, consequently, feeding of the enzyme with small molecule reagents (OFF state to ON state) (Figures 4 and 6). To this end, glucose oxidase (GOx) and myoglobin (Myo) were in situ encapsulated during polymersome formation using a previously published protocol,^[62,63] followed by 5 min of UV irradiation and purification by hollow fiber filtration (HFF) (Figure 3A). The loading efficiency was determined as 3–5% for GOx and 1–2% for Myo (see Supporting Information for further details). From the different assays to study the enzymatic activities of GOx and Myo previously reported,^[62,63] we selected the oxidation

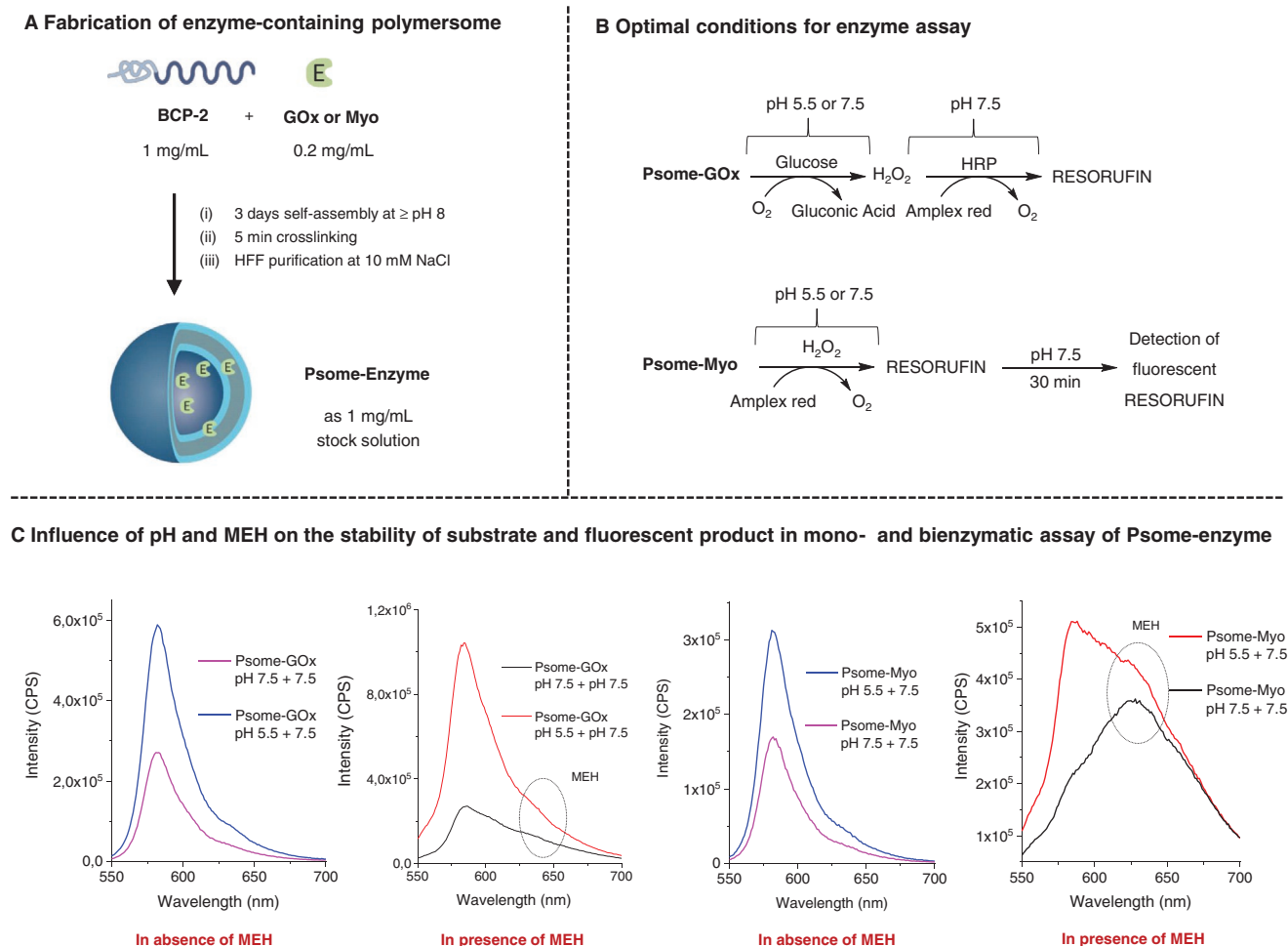
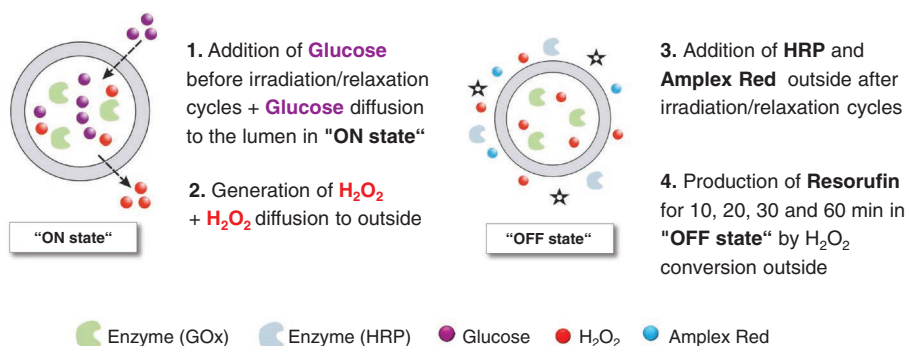


Figure 3. A) Formation of the enzymatic nanoreactor, Psome-enzyme. B) Optimized conditions for enzymatic reactions in each nanoreactor. C) Following the emission of resorufin as a means to study the activity of Psome-GOx (left and center left) and Psome-Myo (center right and right) in the presence or absence of MEH. The reaction was followed by fluorescence spectroscopy ($\lambda_{exc} = 534$ nm, $\lambda_{obs} = 585$ nm). The pH was adjusted manually. All stock solutions used were freshly prepared. Conditions: $C_{Psome-enzyme} = 0.1$ mg BCP per mL ($\ll 0.02$ mg enzyme per mL), $C_{MEH} = 1.66$ mM in MilliQ water with 5% DMSO.

Nanoreactor Psome-GOx

Mechanism through Amplex Red conversion outside in "OFF state"



Nanoreactor Psome-Myo

Mechanism through Amplex Red conversion inside Psome lumen in "OFF state"

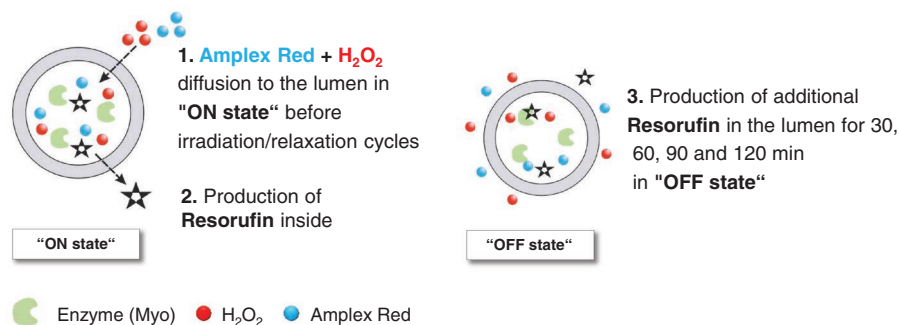


Figure 4. Two concepts of following enzymatic catalysis: Psome-GOx: HRP and Amplex Red are only added to the enzyme assay once MEH/SP photocycling has been completed. Psome-Myo: Amplex Red and H₂O₂ are added to the enzyme assay before photocycling of MEH/SP.

of the non-fluorescent Amplex Red to the easily detectable, fluorescent product, resorufin.^[69,70] Under the conditions employed, the photooxidation of Amplex Red^[71,72] is considered negligible.

Before studying the activity of enzyme-loaded Psomes (Psome-GOx and Psome-Myo in Figure 3) in the presence of MEH (Figures 4 and 6), the influence of MEH on the pH* and membrane collapse properties should be compared for these enzyme-loaded and enzyme-free Psomes under the selected conditions ($C_{\text{loaded Psomes}} = 0.15$ mg BCP per mL, $C_{\text{MEH}} = 1$ mM, 5% DMSO). The following samples were studied: 10% Empty-Psome (0.1 mg BCP per mL) in the presence and absence of 1.0 mM of MEH and enzyme-loaded Psomes, 15% Psome-GOx, and 15% Psome-Myo, (0.15 mg BCP per mL) in the presence of 1.0 mM of MEH (Figure S12, Supporting Information). There is only a marginal shift to lower values for pH* of enzyme-loaded Psomes as found for empty Psomes in the presence of 1 mM of MEH. Thus, in all cases the pH* is in the range 5.90–5.99. Finally, there is no influence of MEH on swelling and collapsing properties of polymersomes in highly diluted solution. These results are essential taking into account that final enzyme activity is limited to pH 7.5 at which polymersomes' membrane is collapsed (OFF state, Figure 6) and to pH 5.5 at which the polymersomes' membrane is open (ON state, Figure 6).

2.5. Activity of Enzymatic Nanoreactors in the Absence of MEH and in the Presence of MEH without Cyclic Irradiation–Relaxation for Probing Key Parameter IV

The enzymatic activity of the enzyme-loaded Psomes could be influenced by the following factors: i) irradiation during the crosslinking process;^[62,68] ii) irradiation of MEH solution to produce light-driven proton transfer; iii) interactions with MEH or other side reactions; iv) pH-dependence of fluorescence. Considering the irradiation results shown in Figures S14 and S15, Supporting Information, only the activity of Myo in the absence of MEH is slightly affected by irradiation. In addition, these control experiments show that the SP form generated in situ by light irradiation has no influence on enzymatic activity. The pH-dependent fluorescence of resorufin (the highest fluorescence intensity at pH 7.5) and MEH (weak signal at pH 7.5) were studied (Figure S10 and S11, Supporting Information), taking into consideration the undesired interfering properties or overlapping of signals. With this in mind, the pH-dependence of the enzymatic assays in the absence and presence of MEH has been tested and the results are shown in Figure 3C (for details on enzymatic assays with free enzymes, see Figures S16 and S17, Supporting Information). In both cases, the enzymatic assay consists of two steps (Figure 3B); the second step was carried out at the optimal pH of 7.5. This

method allows us to study the enzymatic activity under different conditions (including irradiation conditions).

The previously reported assay protocol^[69,73,74] was slightly adapted to our Psome-enzyme system. In the case of Psome-GOx (Figure 3B, top), the assay was based on i) formation of H₂O₂ due to GOx activity and ii) formation of resorufin from Amplex Red in the presence of H₂O₂ due to horseradish peroxidase (HRP) activity. For Psome-Myo (Figure 3B, bottom), we followed the formation of resorufin from Amplex Red and H₂O₂ due to Myo activity. At the detection stage, the pH was adjusted to 7.5 to avoid undesired diffusion from the external environment into the polymersomes' lumen. In this context, the selection of pH values was motivated by the working principle of our previously described pH-switchable enzymatic nano-reactors.^[61,62] For both enzymes, the first step is carried out at pH 5.5 or 7.5, while the second step proceeds at pH 7.5, which is the optimal pH to study the fluorescence of the product resorufin (Figure 3C). The expected higher enzymatic activity is observed at pH 5.5 for the enzyme-loaded Psores. Due to the acidic pH, the Psome-enzyme membrane is swollen and the substrates easily cross the membrane, reacting inside the Psores. The final assay within this experiment series was carried out in the presence of MEH but without irradiation (in the dark). This experiment should also verify that there is no significant interference between resorufin and MEH. As expected (Figure 3C), a significant increase in enzyme activity was detected when the first step was carried out at pH 5.5. Our results show that this assay is highly efficient despite the presence of MEH and the results are similar to those in the absence of MEH. Thus, we can conclude that MEH has no negative influence on the function of enzymatic nano-reactors (Scheme 1; key parameter

IV) and the tested pH regime works well for our enzyme assay. The two configurations of enzymatic reactors (Psome-GOx and Psome-Myo) and the corresponding concepts of following enzymatic activity are shown in Figure 4.

2.6. Structural Parameters of Enzymatic Nanoreactors and Enzyme Locations

The observed enzymatic activity at pH 7.5 (Figure 3) could be attributed to a small percentage of enzyme being anchored to the polymersome membrane and/or adsorbed at the outer surface of the polymersomes. To verify this assumption, asymmetrical flow field flow fractionation (AF4) coupled to light scattering was applied^[75] to evaluate the conformation and shape of the particles and to localize the enzyme within the hybrid structure. Possible locations of the enzyme can be polymersomes' lumen, inner and outer membrane surface, and the interior of the membrane.^[75] To better understand the structure of these species, we plotted the dependence of the radius of gyration, R_g , on the molar mass, M (Figure 5): $R_g \propto M^\nu$, (where ν is the scaling exponent) for the polymersome-enzyme hybrid structures (Psome-GOx and Psome-Myo) and the empty Psores as a reference. For Psome-GOx, a slightly larger R_g can be observed when the enzymes are incorporated within polymersomes' membrane (Figure 5), which could be a result of the differences in the polymersome preparation procedure.

The slope of the plots corresponds to the exponent ν in the scaling law and enables the interpretation of the shape and conformation of the particles. Scaling parameter ν increases slightly from 0.48 (Empty-Psome) to 0.55 (Psome-GOx). Taking

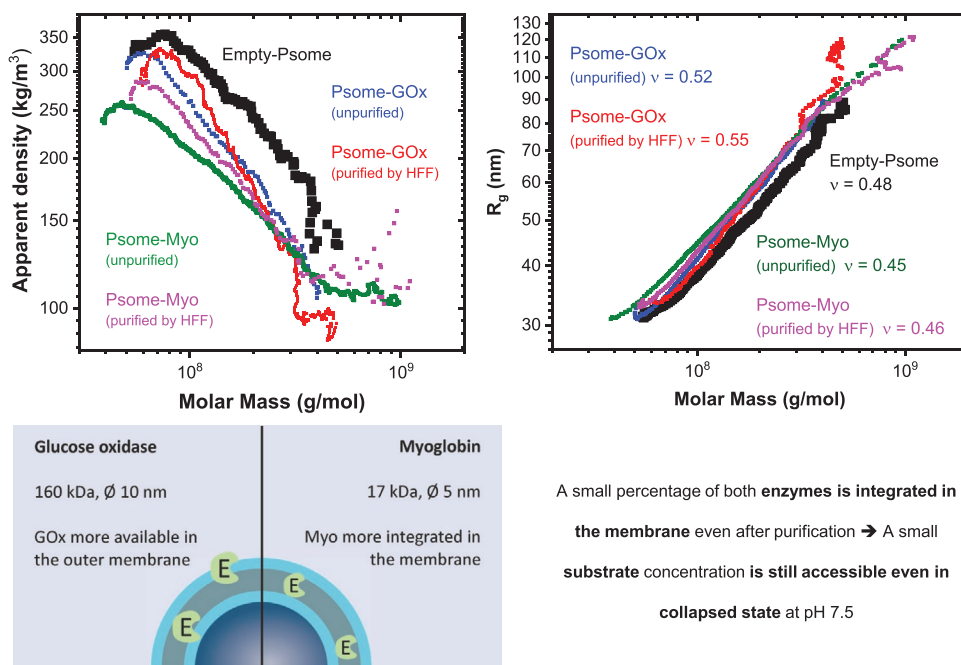


Figure 5. Conformation plot of polymersome derived from AF4 analysis at pH 8. Conditions: 0.5 mg BCP per mL + 0.1 mg mL⁻¹ enzyme. Dependence of the radius of gyration (R_g) on the molar mass (right) and apparent density (left) calculated for polymersomes: empty Psores and Psores loaded in situ with an enzyme (unpurified and purified by HFF). Bottom: Schematic representation of enzyme location within the membrane as found by AF4 conformation and density analysis.

A small percentage of both enzymes is integrated in the membrane even after purification → A small substrate concentration is still accessible even in collapsed state at pH 7.5

into account the theoretical values of ν , values higher than 0.33 toward 0.5 correspond to an object with density lower than a solid sphere. Interactions between proteins and polymer-some membrane lead to transformation of the compact, well-defined BCP assembly into a less homogeneous membrane structure, leading to further increase of ν . At the same time, the corresponding apparent density decreases, clearly confirming the integration of GOx within the membrane. Based on this AF4 study, we conclude that the small activity at pH 7.5 (Figure 3C) can be due to membrane-integrated GOx.

The differences in the scaling parameters of both polymer-some-enzyme systems can be directly attributed to the size of the enzyme used. GOx (160 kDa, \varnothing 10 nm) is much larger than Myo (17 kDa, \varnothing 5 nm). It follows that the incorporation of Myo within the membrane or its attachment onto polymersome surface does not significantly affect the surface of the polymersome. Thus, the scaling parameters found for Psome-Myo and empty Psores are similar. The same behavior is also observed after HFF purification of both systems. At a lower density, however, Myo is also integrated within the membrane.

The above results show that enzymes could not be completely eliminated from the outer membrane surface during HFF purification (Figure 5). It is important to note that a longer crosslinking period (5 min) should fix enzymes integrated within membrane better compared to shorter crosslinking periods (≤ 3 min).^[61,62,66,67,73] Consequently, the substrate can partially access the membrane-integrated enzyme even in the collapsed state of the polymersome membrane (at pH 7.5; Figure 3C). This working hypothesis, as well as the key assumption that the polymersomes' lumen is the main activity site of both enzymes (Figure 4), is verified in the next section.

2.7. Photocontrol of pH-Responsive Enzymatic Nanoreactors Using Light-Triggered Proton Release from MEH

In the last series of experiments designed for establishing the concept of adaptive enzymatic nanoreactors (Scheme 1), reversible switching between ON and OFF states of the enzymatic nanoreactors was realized in the presence of MEH through cyclic application of 3 min irradiation (ON state) and 5 min relaxation in the dark (OFF state). **Figure 6** describes the protocol for light-driven proton transfer in both enzymatic nanoreactors. A batch solution for this series of experiments was prepared by dissolving Psome-enzyme and MEH (1.66 mM) in water with 5% DMSO (for further details, see Experimental Section). The pH of the batch solutions was adjusted to 7.2 (corresponding to the collapsed state of the Psome-enzyme membrane) and excess of glucose (for Psome-GOx; Figure 6A) or a defined concentration of Amplex Red and H₂O₂ (for Psome-Myo; Figure 6B) were added. With these Psome-enzyme solutions, the following samples were prepared (Figure 6): i) sample “non-irradiated”, which acted as a reference; ii) sample “pH changed manually”, where the pH was manually decreased to 5.5 for 9 min and then brought back to 7.5 (through buffer addition); iii) samples “1, 2, or 3 cycle(s) of irradiation”, where each cycle consists of 3 min visible light irradiation followed by 5 min in the dark. At the end of each assay, the OFF state was re-established for each

sample (e.g., after 2 or 3 cycles of MEH/SP switching). Thus, for experiments involving Psome-GOx, the pH was changed to 7.5 and the quantity of H₂O₂ generated in each sample was quantified by fluorescence spectroscopy after the addition of a given amount of HRP and Amplex Red (Figure 6A, bottom). In case of Psome-Myo, the enzymatic activity was studied by following the formation of resorufin (Figure 6B, bottom). The pH values measured for the light-driven proton transfer and dark relaxation for Psome-GOx are summarized in Table S7, Supporting Information.

The last step in the OFF state for all samples (Figure 6) was studied at different times (10, 20, 30, and 60 min for Psome-GOx and 30, 60, 90, and 120 min for Psome-Myo) with two goals in mind: i) to provide Psome-GOx and Psome-Myo with enough time for completing the final enzymatic conversion (in order to enhance the difference between the different numbers of switching cycles) and ii) to demonstrate the impermeability of the membrane in the collapsed state. We found that the optimal times are 10 min for Psome-GOx and 60 min for Psome-Myo (Figure 6). This discrepancy can be explained by the differences in the concentration of the enzymes catalyzing the final step.

Due to the cumulative effect, the fluorescence intensity of resorufin for Psome-GOx (Figure 6A, bottom) is the highest for sample “3 cycles of irradiation” followed by “2 cycles of irradiation” and “1 cycle of irradiation.” Importantly, samples “3 cycles of irradiation” and “pH changed manually” exhibit similar fluorescence intensities. This implies that the reversible opening and closing of the enzymatic nanoreactors by light-triggered pH changes is highly efficient (Figure 2C). For the non-irradiated sample, a certain enzymatic activity for Psome-GOx is found (Figure 6A, bottom, and Figures S20, S21, and S23, Supporting Information) due to the presence of a small amount of membrane/surface-integrated GOx, as discussed above (Figure 5).

The next experiments were aimed at verifying i) the efficiency of light-driven proton transfer and ii) impermeability of the collapsed polymersome membrane after the relaxation process (SP \rightarrow MEH), leading to the OFF state of Psome-GOx. The results (Figure 6A; Figures S20, S21, and S23, Supporting Information) imply the following: First, “non-irradiated” Psome-GOx sample exhibits the desired lack of permeability of the collapsed membrane with low enzyme activity due to very low membrane incorporation of GOx. In this context samples “pH changed manually,” “1 cycle of irradiation,” and “2 cycles of irradiation” show the same level of enzymatic conversion at 10 and 60 min after reaching the final OFF state of the Psome-GOx system, once again emphasizing an impermeable nature of the collapsed membrane, preventing inward diffusion of glucose and outward diffusion of H₂O₂ over a longer time (Figure S23, Supporting Information). On the other hand, the sample “3 cycles of irradiation” shows a slightly increased enzymatic conversion due to a longer feeding time of the first enzymatic reaction and a longer period of release of H₂O₂ from the Psome-GOx (the 9 min-long ON state; enzymatic concept in Figure 4).

For Psome-Myo (Figure 6B, top, and Figures S20, S22, and S24, Supporting Information), the enzymatic conversion is slower than for Psome-GOx (Figure S20, Supporting

Temporal opening of pH-switchable polymersomes' membrane using MEH

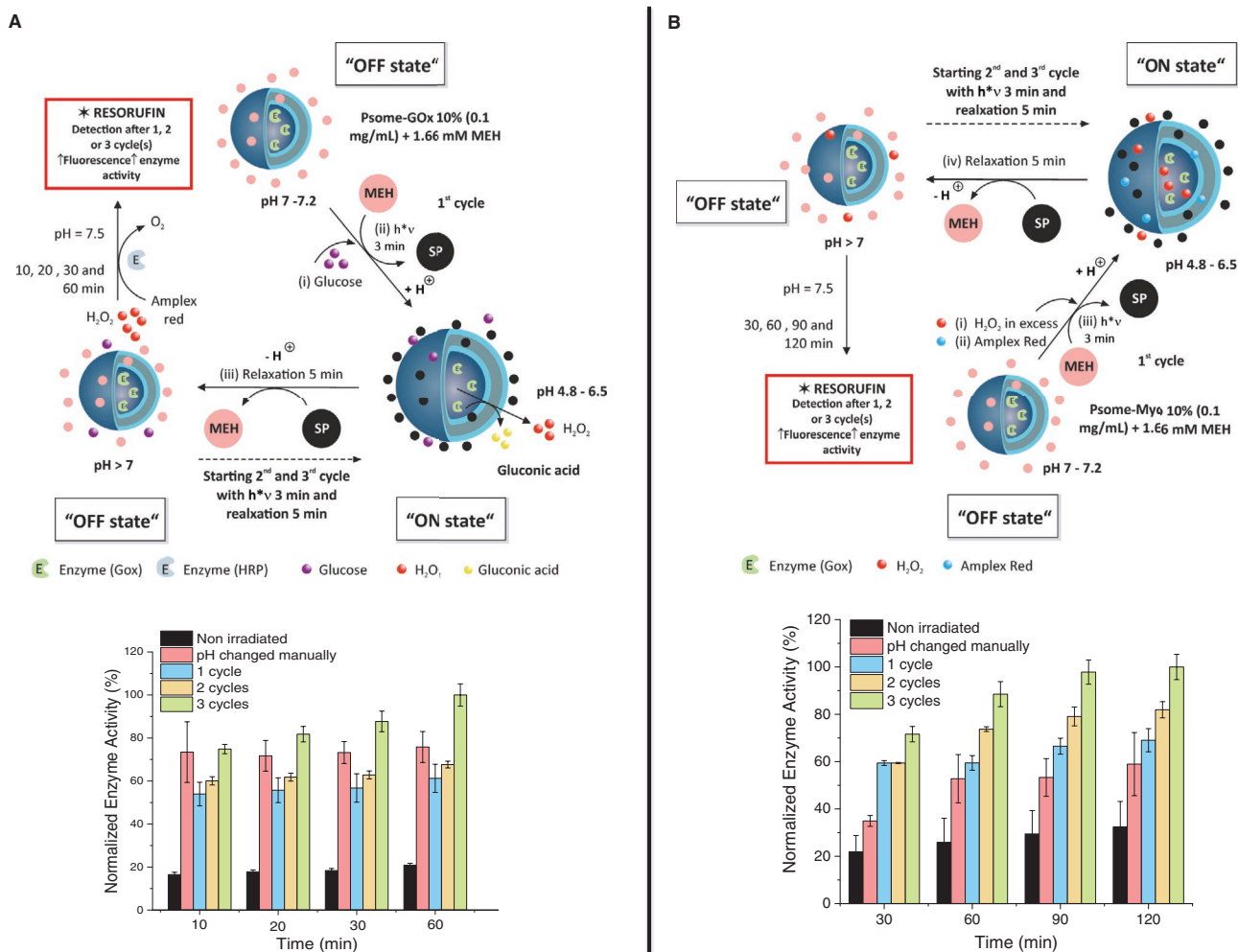


Figure 6. Top panel: Schematic illustration of the final experimental sequences for light-triggered adaptive enzymatic nanoreactors, A) Psome-GOx and B) Psome-Myo. Bottom panel: Normalized enzymatic activity of both nanoreactors after one (blue), two (orange), and three (green) cycles of MEH/SP irradiation-relaxation, with each cycle consisting of 3 min irradiation (ON state) followed by 5 min relaxation in the dark (OFF state). Control experiments: no irradiation (black) and pH changed manually (to pH 5.5 for 9 min, then to pH 7.5) (red). Conditions: $C_{\text{Psome-enzyme}} = 0.1$ mg BCP per mL + $\ll 0.02$ mg enzyme per mL, $C_{\text{MEH}} = 1.66$ mM in MilliQ water with 5% DMSO. Each experiment was carried out at least in triplicate; enzymatic activity determined at different time points after reaching the final OFF state of the enzymatic nanoreactor ($\lambda_{\text{exc}} = 534$ nm, $\lambda_{\text{obs}} = 585$ nm). All stock solutions used were freshly prepared. Initial pH = 7.2; pH after three irradiation-relaxation cycles = 7 (see Table S7, Supporting Information).

Information), as explained above by the different configurations (Figure 4). Sample “non-irradiated” shows a nearly constant, low enzymatic activity for collapsed polymersome membrane, most likely due to a small amount of Myo integrated within the membrane (Figure 5). It is important to point out that the differences in the enzymatic conversion for different irradiation cycles might be due to potential photooxidation of Amplex Red.^[71,72] However, this possibility was ruled out above (Figure S15B, Supporting Information). Overall, these results confirm the presence of non-permeable, collapsed polymersome membrane over time and the critical role of light-driven proton transfer. Moreover, the results strengthen the working hypothesis regarding the major and minor location of both enzymes in Psome-GOx and Psome-Myo (Section 2.6).

3. Conclusions

We demonstrated the design and fabrication of adaptive enzymatic nanoreactors that drive a catalytic reaction by temporal control of the membrane permeability through a reversibly switchable light-driven proton transfer. Protonated MEH was used as the photoactive proton donor undergoing light-driven transformation to spiropyran (SP) with the release of protons, which rapidly protonate the nanoreactor membrane, rendering it permeable for substrates of enzymatic reactions. These permeable membranes return to their initial, impermeable state rapidly when the light stimulus is withdrawn due to the thermal relaxation of SP back to MEH. Several key parameters, including crosslinking density of the polymersome membrane

and concentrations of polymersome and MEH, have been investigated to determine the optimal conditions for cyclic, temporal switching of the enzymatic nanoreactors in mono- and bienzymatic reactions through light-driven proton transfer. Using this functional principle, several ON–OFF cycles could be accomplished in a reproducible way. Under exposure to visible light, higher amounts of the product could be obtained. In the OFF state of the enzymatic nanoreactors, the membrane was collapsed, preventing inward diffusion of the substrates and outward diffusion of the products. This strategy provides a straightforward solution for the development of catalytic nanocompartments efficiently producing desired molecules in a spatiotemporally controlled and stimuli-responsive manner with high potential in areas such as catalysis, analytical chemistry, and systems biology.

4. Experimental Section

Materials: Poly(ethylene glycol) methyl ether (MeO-PEG-OH; $M_n = 2000 \text{ g}\cdot\text{mol}^{-1}$; $M_w/M_n = 1.05$), 2,2'-bipyridine, 4-aminobutanol, 2-(diethylamino)ethyl methacrylate (DEAEM), methacryloyl chloride, 2-bromoisobutyl bromide, 2-aminoethanol, copper(I) bromide, aluminum oxide (neutral, activated), GOx from *Aspergillus niger* (essentially salt-free, lyophilized powder), Myo from equine skeletal muscle (essentially salt-free, lyophilized powder), hydrogen peroxide solution (30%), resorufin, phosphate buffered saline (tablet), sodium hydroxide, magnesium sulfate, D-(+)-glucose, and HRP were purchased from Sigma-Aldrich. 3,4-Dimethylmaleic acid anhydride, toluene, THF, ethyl acetate, and chloroform-d were purchased from Acros Organics. Hydrochloric acid (37%), *n*-hexane, and silica gel were purchased from Merck (Germany). Amplex Red was purchased from Thermo Fischer. Anhydrous 2-butanone (Fluka), triethylamine (Fluka), and anhydrous tetrahydrofuran (THF) (Sigma-Aldrich) were stored over molecular sieves. Protonated MEH was synthesized and characterized according to a previously published procedure.^[17,76,77] All analytical methods, assays, and instruments used for characterization are described in the Supporting Information.

Fabrication of Materials: Details on the syntheses and characterization of the BCP and the preparation of empty and enzyme-loaded Psomes can be found in the Supporting Information (Figures S1 and S, Tables S1 and S2, Supporting Information). Stock solutions: 1 mg BCP per mL of Psome-GOx (encapsulation efficiency of GOx around 3–5%), 1 mg BCP per mL of Psome-Myo (encapsulation efficiency of Myo around 1–2%), 0.2 mg mL⁻¹ of HRP, 0.02 mg mL⁻¹ glucose, 0.02 mg mL⁻¹ Amplex Red, and 0.02 M H₂O₂. The solution of MEH was ultrasonicated and then irradiated with a Hg lamp for 3 min to facilitate the dissolution of MEH (final concentration, 2.07 mM). GOx activity assay for Psome-GOx (in the presence of MEH) using light as the stimulus for several short-term cycles: Using the MEH stock solution (2.07 mM; prepared as described above) and the stock solution of Psome-GOx (prepared from 1 mg BCP per mL with 0.2 mg GOx per mL), 10 mL of solution of Psome-GOx and MEH was prepared with 10 mM NaCl; final concentration = 0.1 mg mL⁻¹ of Psome-GOx and 1.66 mM of MEH (in water with 5% DMSO). This batch solution with pH 7.2 (the starting point for light-driven proton transfer experiments as shown in Figure 6A) was divided into five portions: a) Sample 1—“non-irradiated”: To 2 mL of the solution, 2.25 μL of glucose solution (0.02 mg mL⁻¹) was added. After 9 min, 3.2 μL of Amplex Red solution (0.02 mg mL⁻¹) and 55 μL of HRP solution (0.2 mg mL⁻¹) were added and fluorescence spectra were recorded after 10, 20, 30, and 60 min. b) Sample 2—“pH changed manually”: To 2 mL of the solution (pH manually adjusted to 5.5), 2.25 μL of glucose solution (0.02 mg mL⁻¹) was added. After 9 min, the pH of the solution was re-adjusted to 7.5 and 3.2 μL of Amplex Red solution (0.02 mg mL⁻¹) and 55 μL of HRP solution (0.2 mg mL⁻¹)

were added and fluorescence spectra were recorded after 10, 20, 30, and 60 min. c) Samples 3–5—“1 cycle”, “2 cycles”, and “3 cycles of irradiation”: 2.25 μL of glucose solution (0.02 mg mL⁻¹) was added to 2 mL of each sample. The samples were irradiated and allowed to relax in the dark for 1, 2, or 3 cycle(s) (each cycle: 3 min of irradiation followed by 5 min of relaxation). After 1, 2, or 3 cycle(s) of irradiation, the final pH was adjusted to 7.5 and 3.2 μL of Amplex Red solution (0.02 mg mL⁻¹) and 55 μL of HRP solution (0.2 mg mL⁻¹) were added and fluorescence spectra were recorded after 10, 20, 30, and 60 min.

Myoglobin Activity Assay for Psome-Myo (in the Presence of MEH) Using Light as Stimuli for Several Short-Term Cycles: Using the MEH stock solution (2.07 mM; prepared as described above) and stock solution of Psome-Myo (prepared from 1 mg BCP per mL with 0.2 mg Myo per mL), 10 mL of solution of Psome-Myo and MEH were prepared with 10 mM NaCl; final concentration = 0.1 mg mL⁻¹ of Psome-Myo and 1.66 mM of MEH (in water with 5% DMSO). This batch solution with pH 7.2 (starting point for the light-driven proton transfer experiments as shown in Figure 6B) was divided into five portions: a) Sample 1—“non-irradiated”: To 2 mL of the solution, 60 μL of H₂O₂ solution (0.02 M) and 60 μL of Amplex Red solution (0.02 mg mL⁻¹) were added. After 10 min, 2 mL of a 10 mM PBS solution at pH 7.5 were added. The fluorescence spectra were recorded after 30, 60, 90, and 120 min. b) Sample 2—“pH changed manually”: To 2 mL of the solution (pH manually adjusted to 5.5), 60 μL of H₂O₂ solution (0.02 M) and 60 μL of Amplex Red solution (0.02 mg mL⁻¹) were added. After 10 min, 2 mL of a 10 mM PBS solution at pH 7.5 were added. The fluorescence spectra were recorded after 30, 60, 90, and 120 min. c) Samples 3–5—“1 cycle”, “2 cycles”, and “3 cycles of irradiation”: 60 μL of H₂O₂ solution (0.02 M) and 60 μL of Amplex Red solution (0.02 mg mL⁻¹) were added to 2 mL of each sample and the resulting solutions were subjected to 1, 2, or 3 irradiation–relaxation cycle(s) (each cycle: 3 min of irradiation followed by 5 min of relaxation). After 1, 2, or 3 cycle(s) of irradiation, the final pH was adjusted to 7.5 by adding 2 mL of a 10 mM PBS solution at pH 7.5 and fluorescence spectra were recorded after 30, 60, 90, and 120 min.

Supporting Information

Supporting Information is available from the Wiley Online Library or from the author.

Acknowledgements

S.M. has been supported by a grant from Fundación Alfonso Martín Escudero (Spain government). P.S. has been supported by grant from DAAD India IIT Master Sandwich Programme funded by DAAD. R.K. acknowledges support from the Minerva Foundation with funding from the Federal German Ministry for Education and Research. The authors would like to thank Dr. Petr Formanek for carrying out cryo-TEM. Correction added on September 24, 2020, after first online publication: Projekt Deal funding statement has been added.

Open access funding enabled and organized by Projekt DEAL.

Conflict of Interest

The authors declare no conflict of interest.

Keywords

light-driven proton transfer, ON–OFF systems, out-of-equilibrium systems, photoacids, polymersomes

Received: April 2, 2020

Revised: May 25, 2020

Published online: August 11, 2020

- [1] D. Baazov, X. Wang, D. Khananshvili, *Biochemistry* **1999**, *38*, 1435.
- [2] F. Ciardelli, D. Fabbri, O. Pieroni, A. Fissi, *J. Am. Chem. Soc.* **1989**, *111*, 3470.
- [3] P. V. Jog, M. S. Gin, *Org. Lett.* **2008**, *10*, 3693.
- [4] R. F. Khairutdinov, J. K. Hurst, *Langmuir* **2004**, *20*, 1781.
- [5] R. Klajn, P. J. Wesson, K. J. M. Bishop, B. A. Grzybowski, *Angew. Chem., Int. Ed.* **2009**, *48*, 7035.
- [6] P. K. Kundu, S. Das, J. Ahrens, R. Klajn, *Nanoscale* **2016**, *8*, 19280.
- [7] Y. Lei, J. K. Hurst, *Langmuir* **1999**, *15*, 3424.
- [8] M. Grzelczak, L. M. Liz-Marzán, R. Klajn, *Chem. Soc. Rev.* **2019**, *48*, 1342.
- [9] O. F. Mohammed, D. Pines, J. Dreyer, E. Pines, E. T. J. Nibbering, *Science* **2005**, *310*, 83.
- [10] T. Seki, K. Ichimura, *J. Phys. Chem.* **1990**, *94*, 3769.
- [11] O. A. Sytina, D. J. Heyes, C. N. Hunter, M. T. Alexandre, I. H. M. van Stokkum, R. van Grondelle, M. L. Groot, *Nature* **2008**, *456*, 1001.
- [12] P. Wan, D. Shukla, *Chem. Rev.* **1993**, *93*, 571.
- [13] J. D. Winkler, K. Deshayes, B. Shao, *J. Am. Chem. Soc.* **1989**, *111*, 769.
- [14] D. S. Achilleos, T. A. Hatton, M. Vamvakaki, *J. Am. Chem. Soc.* **2012**, *134*, 5726.
- [15] S. S. Babu, V. K. Praveen, A. Ajayaghosh, *Chem. Rev.* **2014**, *114*, 1973.
- [16] S. Jia, W.-K. Fong, B. Graham, B. J. Boyd, *Chem. Mater.* **2018**, *30*, 2873.
- [17] R. Klajn, *Chem. Soc. Rev.* **2014**, *43*, 148.
- [18] H. Q. Peng, L. Y. Niu, Y.-Z. Chen, L. Z. Wu, C.-H. Tung, Q. Z. Yang, *Chem. Rev.* **2015**, *115*, 7502.
- [19] D. H. Qu, Q. C. Wang, Q. W. Zhang, X. Ma, H. Tian, *Chem. Rev.* **2015**, *115*, 7543.
- [20] T. Bian, Z. Chu, R. Klajn, *Adv. Mater.* **2020**, *32*, 1905866.
- [21] D. Su, C. L. Teoh, L. Wang, X. Liu, Y. T. Chang, *Chem. Soc. Rev.* **2017**, *46*, 4833.
- [22] W. Szymanski, D. Yilmaz, A. Koçer, B. L. Feringa, *Acc. Chem. Res.* **2013**, *46*, 2910.
- [23] G. G. Dias, A. King, F. de Moliner, M. Vendrell, E. N. da Silva Jr., *Chem. Soc. Rev.* **2018**, *47*, 12.
- [24] E. Rideau, R. Dimova, P. Schwille, F. R. Wurm, K. Landfester, *Chem. Soc. Rev.* **2018**, *47*, 8572.
- [25] V. Balzani, A. Credi, M. Venturi, *Chem. Soc. Rev.* **2009**, *38*, 1542.
- [26] B. L. Feringa, *Angew. Chem., Int. Ed.* **2017**, *56*, 11060.
- [27] Q. Shi, Z. Meng, J. F. Xiang, C. F. Chen, *Chem. Commun.* **2018**, *54*, 3536.
- [28] S. Silvi, A. Arduini, A. Pochini, A. Secchi, M. Tomasulo, F. M. Raymo, M. Baroncini, A. Credi, *J. Am. Chem. Soc.* **2007**, *129*, 13378.
- [29] S. Kwangmettata, T. Kudernac, *Chem. Commun.* **2018**, *54*, 5311.
- [30] J. Moratz, A. Samanta, J. Voskuhl, S. K. Mohan-Nalluri, B. J. Ravoo, *Chem. - Eur. J.* **2015**, *21*, 3271.
- [31] O. Rifaie-Graham, S. Ulrich, N. F. B. Galensowske, S. Balog, M. Chami, D. Rentsch, J. R. Hemmer, J. R. de Alaniz, L. F. Boesel, N. Bruns, *J. Am. Chem. Soc.* **2018**, *140*, 8027.
- [32] X. Wang, J. Hu, G. Liu, J. Tian, H. Wang, M. Gong, S. Liu, *J. Am. Chem. Soc.* **2015**, *137*, 15262.
- [33] D. Xia, G. Yu, J. Li, F. Huang, *Chem. Commun.* **2014**, *50*, 3606.
- [34] Y. Xiong, A. V. Jentzsch, J. W. Osterrieth, E. Sezgin, I. V. Sazanovich, K. Reglinski, S. Galiani, A. W. Parker, C. Eggeling, H. L. Anderson, *Chem. Sci.* **2018**, *9*, 3029.
- [35] A. Samanta, M. C. A. Stuart, B. J. Ravoo, *J. Am. Chem. Soc.* **2012**, *134*, 19909.
- [36] R. Merindol, A. Walther, *Chem. Soc. Rev.* **2017**, *46*, 5588.
- [37] H. Che, J. C. M. van Hest, *J. Mater. Chem. B* **2016**, *4*, 4632.
- [38] Y. S. Kandasamy, J. Cai, J. G. Ottaviano, K. A. Smith, A. N. Williams, J. Moore, K. M. Louis, L. Selzler, A. Beler, T. Okwuonu, *Org. Biomol. Chem.* **2016**, *14*, 296.
- [39] U. Kauscher, A. Samanta, B. J. Ravoo, *Org. Biomol. Chem.* **2014**, *12*, 600.
- [40] M. A. Watson, S. L. Cockcroft, *Chem. Soc. Rev.* **2016**, *45*, 6118.
- [41] H. Che, S. Cao, J. C. M. van Hest, *J. Am. Chem. Soc.* **2018**, *140*, 5356.
- [42] K. Schulten, P. Tavan, *Nature* **1978**, *272*, 85.
- [43] J. Barber, B. Andersson, *Nature* **1994**, *370*, 31.
- [44] A. Taglieber, F. Schulz, F. Hollmann, M. Rusek, M. T. Reetz, *Chem-BioChem* **2008**, *9*, 565.
- [45] G. Wang, K. Castiglione, *Catalysts* **2018**, *9*, 12.
- [46] N. Ritzmann, J. Thoma, S. Hirschi, D. Kalbermatter, D. Fotiadis, D. J. Müller, *Biophys. J.* **2017**, *113*, 1181.
- [47] J. Gaitzsch, S. Hirschi, S. Freimann, D. Fotiadis, W. Meier, *Nano Lett.* **2019**, *19*, 2503.
- [48] D. Hvasanov, J. R. Peterson, P. Thordarson, *Chem. Sci.* **2013**, *4*, 3833.
- [49] D. Wendell, J. Todd, C. Montemagno, *Nano Lett.* **2010**, *10*, 3231.
- [50] X. Feng, Y. Jia, P. Cai, J. Fei, J. Li, *ACS Nano* **2016**, *10*, 556.
- [51] Z. Shi, P. Peng, D. Strohecker, Y. Liao, *J. Am. Chem. Soc.* **2011**, *133*, 14699.
- [52] J. Vallet, J. C. Micheau, C. Coudret, *Dyes Pigm.* **2016**, *125*, 179.
- [53] Y. S. Nam, I. Yoo, O. Yarimaga, I. S. Park, D. H. Park, S. Song, J. M. Kim, C. W. Lee, *Chem. Commun.* **2014**, *50*, 4251.
- [54] T. Halbritter, C. Kaiser, J. Wachtveitl, A. Heckel, *J. Org. Chem.* **2017**, *82*, 8040.
- [55] P. K. Kundu, D. Samanta, R. Leizrowice, B. Margulis, H. Zhao, M. Börner, T. Udayabhaskararao, D. Manna, R. Klajn, *Nat. Chem.* **2015**, *7*, 646.
- [56] L. Kuang, D. A. Fernandes, M. O'Halloran, W. Zheng, Y. Jiang, V. Ladizhansky, L. S. Brown, H. Liang, *ACS Nano* **2014**, *8*, 537.
- [57] L. Zhang, L. Dai, Y. Rong, Z. Liu, D. Tong, Y. Huang, T. Chen, *Langmuir* **2015**, *31*, 1164.
- [58] E. Cabane, V. Malinova, S. Menon, C. G. Palivan, W. Meier, *Soft Matter* **2011**, *7*, 9167.
- [59] Z. Sun, G. Liu, J. Hu, S. Liu, *Biomacromolecules* **2018**, *19*, 2071.
- [60] M. A. Yassin, D. Appelhans, R. Wiedemuth, P. Formanek, S. Boye, A. Lederer, A. Temme, B. Voit, *Small* **2015**, *11*, 1580.
- [61] J. Gaitzsch, D. Appelhans, L. Wang, G. Battaglia, B. Voit, *Angew. Chem., Int. Ed.* **2012**, *51*, 4448.
- [62] D. Grafe, J. Gaitzsch, D. Appelhans, B. Voit, *Nanoscale* **2014**, *6*, 10752.
- [63] X. Liu, P. Formanek, B. Voit, D. Appelhans, *Angew. Chem., Int. Ed.* **2017**, *56*, 16233.
- [64] M. Save, J. V. M. Weaver, S. P. Armes, P. McKenna, *Macromolecules* **2002**, *35*, 1152.
- [65] R. T. Pearson, N. J. Warren, A. L. Lewis, S. P. Armes, G. Battaglia, *Macromolecules* **2013**, *46*, 1400.
- [66] R. Ccorahua, S. Moreno, H. Gumz, K. Sahre, B. Voit, D. Appelhans, *RSC Adv.* **2018**, *8*, 25436.
- [67] H. Gumz, T. H. Lai, B. Voit, D. Appelhans, *Polym. Chem.* **2017**, *8*, 2904.
- [68] J. Gaitzsch, I. Canton, D. Appelhans, G. Battaglia, B. Voit, *Biomacromolecules* **2012**, *13*, 4188.
- [69] H. H. Gorris, D. R. Walt, *J. Am. Chem. Soc.* **2009**, *131*, 6277.
- [70] T. Y. D. Tang, D. Cecchi, G. Fracasso, D. Accardi, A. Coutable-Pennarun, S. S. Mansy, A. W. Perriman, J. L. R. Anderson, S. Mann, *ACS Synth. Biol.* **2018**, *7*, 339.
- [71] B. Zhao, F. A. Summers, R. P. Mason, *Free Radical Biol. Med.* **2012**, *53*, 1080.
- [72] B. Zhao, K. Ranguelova, J. Jiang, R. P. Mason, *Free Radical Biol. Med.* **2011**, *51*, 153.
- [73] H. Bäumler, R. Georgieva, *Biomacromolecules* **2010**, *11*, 1480.
- [74] Y. Elani, R. V. Law, O. Ces, *Nat. Commun.* **2014**, *5*, 5305.
- [75] H. Gumz, S. Boye, B. Ilysan, V. Krönert, P. Formanek, B. Voit, A. Lederer, D. Appelhans, *Adv. Sci.* **2019**, *6*, 1801299.
- [76] D. Samanta, D. Galaktionova, J. Gemen, L. J. W. Shimon, Y. Diskin-Posner, L. Avram, P. Král, R. Klajn, *Nat. Commun.* **2018**, *9*, 641.
- [77] D. Samanta, R. Klajn, *Adv. Opt. Mater.* **2016**, *4*, 1373.